

# Compressible Turbulent Plane Couette Flow with Variable Heat Transfer Based on von Kármán Model

R. H. KORKEGI\* AND R. A. BRIGGS†  
Aerospace Research Labs.,  
Wright-Patterson Air Force Base, Ohio

## Introduction

IN an earlier paper<sup>1</sup> the present authors presented a solution to the problem of compressible turbulent plane Couette flow for the symmetrical case of equal temperature, and therefore equal heat transfer, at both walls. The von Kármán turbulent model was used in Ref. 1 on the basis of its good agreement with the low speed measurements of Robertson<sup>2</sup> and the fact that compressible turbulent boundary-layer theories based on this model give best agreement with measurements on flat plates for both the adiabatic and non-adiabatic cases according to the survey of Spalding and Chi.<sup>3</sup>

Interest in compressible, turbulent plane Couette flow stems from the use of slipper bearings to support rocket-boosted sleds at speeds of several 1000 fps<sup>4</sup> e.g., the test track at Holloman Air Force Base, and also possible application to very high-speed tube-guided vehicles.

In the present paper, the solution for compressible turbulent-plane Couette flow based on the von Kármán model is extended to the general case of arbitrary wall temperature. A more detailed study will be given in a forthcoming Aerospace Research Labs' report.

## Governing Equations

With shear constant,  $\tau_w$ , for Couette flow, and neglecting the laminar contribution, the von Kármán mixing length model leads to the differential equation reflecting conservation of momentum<sup>1</sup>

$$d^2u^+/dy^{+2} + \kappa(\rho/\rho_1)^{1/2}(du^+/dy^+)^2 = 0 \quad (1)$$

whose general solution with the boundary condition  $u^+(y^+ = 0) = 0$ , is

$$\frac{E}{\kappa} y^+ = \int_0^{u^+} \exp \left\{ \kappa \int_0^{\xi=u^+} \left( \frac{\rho}{\rho_1} \right)^{1/2} d\xi \right\} du^+ \quad (2)$$

where

$$y^+ = \frac{u_\tau y}{\nu_1}; \quad u^+ = \frac{u}{u_\tau}; \quad u_\tau = \left( \frac{\tau_w}{\rho_1} \right)^{1/2}$$

Time average values are used and  $E/\kappa$  is a constant of integration expressed in the notation of turbulent boundary-layer theories. Following Ref. 1,  $E$  is taken as 8.8, which value gave best agreement with incompressible data, and the mixing length constant  $\kappa = 0.4$ . The subscript 1 denotes the value at a wall, and will be defined later for stationary and moving walls.

As Couette flow is generated by the relative motion of two parallel walls, the procedure followed is to use Eq. (2) which is a "law of the wall"-type equation, to obtain the velocity distribution at each wall separately, and then to determine the matching point of the two profiles with the requirement that the velocities and their slopes must be equal at this point.

A sketch of the flow and pertinent parameters is given in Fig. 1 with the subscript  $w$  denoting values at the stationary

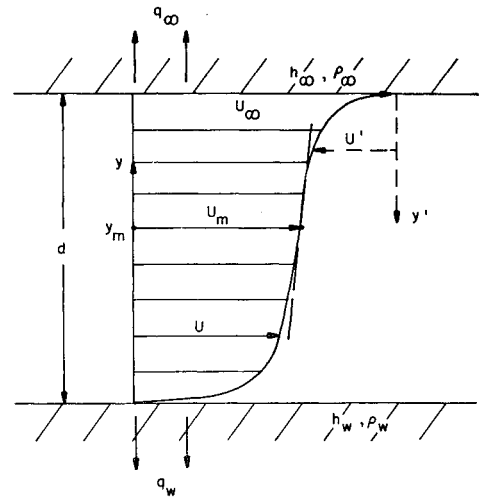


Fig. 1 Sketch of turbulent plane Couette flow.

wall, and  $\infty$ , at the moving wall. The Couette flow Reynolds number and skin-friction coefficient are defined in terms of conditions at the moving wall as follows

$$Re_d = \rho_\infty u_\infty d / \mu_\infty, \quad C_f = 2\tau_w / \rho_\infty$$

Note that  $C_f$ , by definition, has the same value at both walls. Also, the above definitions are necessarily different from those used in Ref. 1 which were based on flow midpoint values.

Applying Eq. (2) to the flow adjacent to the stationary wall, one can write

$$\rho_1 = \rho_w; \quad y^+ = \left( \frac{\tau_w}{\rho_w} \right)^{1/2} \left( \frac{y}{\nu_w} \right) = \left( \frac{C_f}{2} \right)^{1/2} Re_d \left( \frac{\nu_\infty}{\nu_w} \right) \left( \frac{\rho_\infty}{\rho_w} \right)^{1/2} \left( \frac{y}{d} \right)$$

$$u^+ = \frac{u}{(\tau_w/\rho_w)^{1/2}} = \left( \frac{2}{C_f} \right)^{1/2} \left( \frac{\rho_w}{\rho_\infty} \right)^{1/2} \left( \frac{u}{u_\infty} \right)$$

and thus

$$\frac{E}{\kappa} \left( \frac{C_f}{2} \right) Re_d \left( \frac{y}{d} \right) = \left( \frac{\mu_w}{\mu_\infty} \right) \int_0^{\bar{u}} \exp \left\{ \kappa \left( \frac{2}{C_f} \right)^{1/2} \times \int_0^{\eta=\bar{u}} \left( \frac{\rho}{\rho_\infty} \right)^{1/2} d\eta \right\} d\bar{u} \quad (3)$$

where  $\bar{u} = u/u_\infty$ . Equation (3) is valid from  $y = 0$  to a matching point,  $y_m$ , discussed previously.

Similarly, for the moving wall one obtains

$$\rho_1 = \rho_\infty; \quad y^+ = (\tau_w/\rho_\infty)^{1/2} y'/\nu_\infty = (C_f/2)^{1/2} Re_d (y'/d)$$

$$u^+ = u'/(\tau_w/\rho_\infty)^{1/2} = (2/C_f)^{1/2} (u'/u_\infty)$$

and thus

$$\frac{E}{\kappa} \left( \frac{C_f}{2} \right) Re_d \left( \frac{y'}{d} \right) = \int_0^{\bar{u}'} \exp \left\{ \kappa \left( \frac{2}{C_f} \right)^{1/2} \times \int_0^{\eta=\bar{u}'} \left( \frac{\rho}{\rho_\infty} \right)^{1/2} d\eta \right\} d\bar{u}' \quad (4)$$

where  $(y'/d) = 1 - (y/d)$  and  $\bar{u}' = (u'/u_\infty) = 1 - \bar{u}$ .

Equation (4) is valid from the matching point  $y = y_m$  to  $y = d$ .

The density ratio  $\rho/\rho_\infty$  is related to the velocity distribution by the equation of conservation of energy,  $q - \tau u = q_w$ , which, upon integration, yields<sup>1</sup>

$$h = h_w - Pr_\epsilon (q_w/\tau_w) u - Pr_\epsilon (u^2/2) \quad (5)$$

Received July 23, 1969; revision received December 15, 1969.

\* Director, Hypersonic Research Laboratory.

† Visiting Research Associate, Ohio State University Research Foundation (deceased).

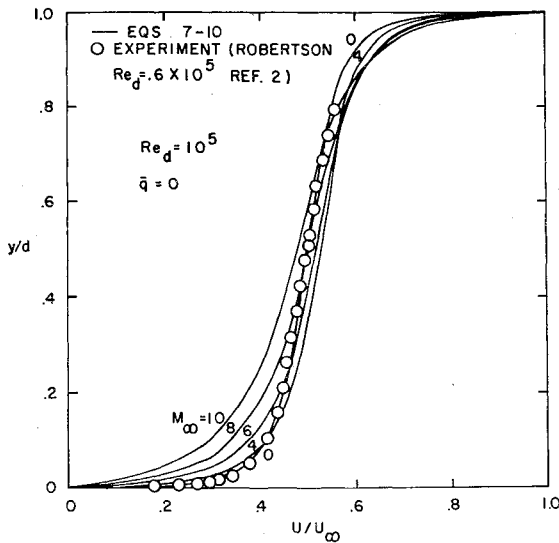


Fig. 2 Velocity profiles for adiabatic stationary wall and various Mach numbers at  $Re_d = 10^5$ .

in which the laminar contribution is neglected and  $Pr_\epsilon = C_p \mu_\epsilon / k_\epsilon$  is a turbulent Prandtl number.

Introducing Mach number  $M_\infty$  based on moving wall velocity and enthalpy, in terms of the parameter  $m^2 = [(\gamma - 1)/2] M_\infty^2 = u_\infty^2 / 2h_\infty$ , and a parameter reflecting the fractional heat due to viscous dissipation transferred to the stationary wall,  $\bar{q} = -2q_w / \tau_w u_\infty$ , Eq. (5) can be written

$$\rho_\infty / \rho = T / T_\infty = h / h_\infty = 1 + Pr_\epsilon m^2 (1 - \bar{q} + \bar{q}\bar{u} - \bar{u}^2) \quad (6)$$

assuming a perfect gas and noting that  $p = \text{constant}$  for Couette flow. Utilizing Eq. (6),  $\bar{q}$  can be expressed in the form of an enthalpy potential

$$\bar{q} = (h_r - h_w) / (h_r - h_\infty)$$

where  $h_w$  is the enthalpy at the stationary wall ( $\bar{u} = 0$ ) and  $h_r$ , its adiabatic value ( $\bar{q} = 0$ ).

#### Velocity Profiles and Friction Law

Substituting Eq. (6) into Eq. (3), integrating, and assuming a linear viscosity-temperature relation— $\mu \sim T$ —for  $\mu_w / \mu_\infty$ , and  $Pr_\epsilon = 1$ , one obtains for the velocity profile adjacent to the stationary wall

$$[1 + (m^2/\kappa)(C_f/2)][E(C_f/2)^{1/2} Re_d (y/d)] = [1 + m^2(1 - \bar{q})] \{ [1 + m^2(1 - \bar{q} + \bar{q}\bar{u} - \bar{u}^2)]^{1/2} + (m^2/\kappa)(C_f/2)^{1/2} (\bar{u} - \bar{q}/2) \} \times \exp \{ (\kappa/m)(2/C_f)^{1/2} \times \{ \sin^{-1} m(\bar{u} - \bar{q}/2) / [1 + m^2(1 - \bar{q}/2)^2]^{1/2} + \sin^{-1} m(\bar{q}/2) / [1 + m^2(1 - \bar{q}/2)^2]^{1/2} \} \} - [1 + m^2(1 - \bar{q})]^{1/2} + m^2/\kappa(C_f/2)^{1/2} \bar{q}/2 \quad (7)$$

for

$$0 \leq y \leq y_m; \quad 0 \leq \bar{u} \leq \bar{u}_m$$

In the limit as  $m \rightarrow 0$ , Eq. (7) reduces to the well-known incompressible form

$$u = 1/\kappa(C_f/2)^{1/2} \ln \{ E(C_f/2)^{1/2} Re_d y/d + 1 \}; \quad 0 \leq y/d \leq \frac{1}{2}$$

Similarly, from Eq. (4) one obtains the velocity profile adjacent to the moving wall re-expressed in terms of co-

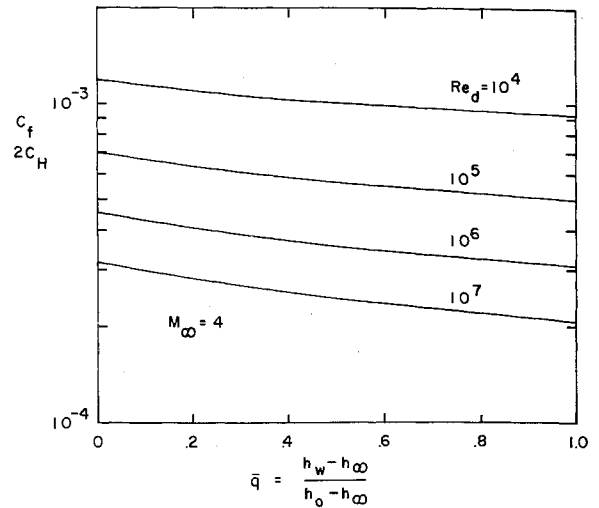


Fig. 3 Influence of wall enthalpy on skin friction and heat-transfer coefficients at  $M_\infty = 4$ .

ordinates fixed to the stationary wall.

$$[1 + (m^2/\kappa)C_f/2][E(C_f/2)^{1/2} Re_d (1 - y/d)] = \{ [1 + m^2(1 - \bar{q} + \bar{q}\bar{u} - \bar{u}^2)]^{1/2} - m^2/\kappa(C_f/2)^{1/2} \times (\bar{u} - \bar{q}/2) \} \times \exp \{ (\kappa/m)(2/C_f)^{1/2} \{ \sin^{-1} m(1 - \bar{q}/2) / [1 + m^2(1 - \bar{q}/2)^2]^{1/2} - \sin^{-1} m(\bar{u} - \bar{q}/2) / [1 + m^2(1 - \bar{q}/2)^2]^{1/2} \} \} - 1 + m^2/\kappa(C_f/2)^{1/2} (1 - \bar{q}/2) \quad (8)$$

for

$$y_m \leq y \leq d; \quad \bar{u}_m \leq \bar{u} \leq 1$$

For the complete determination of the velocity distribution, the skin-friction coefficient and the matching point ( $y_m$  or  $u_m$ ) must be obtained. They are found by equating, respectively, the velocities, and the velocity derivatives between Eqs. (7) and (8). Thus, from the former operation and upon simplification, the skin-friction law is

$$[1 + (m^2/\kappa)C_f/2]E(C_f/2)^{1/2} Re_d = 2[1 + m^2(1 - \bar{q})]^{1/2} \times [1 + m^2(1 - \bar{q} + \bar{q}\bar{u}_m - \bar{u}_m^2)]^{1/2} \times \exp \{ (\kappa/2m)(2/C_f)^{1/2} \times \{ \sin^{-1} m(\bar{q}/2) / [1 + m^2(1 - \bar{q}/2)^2]^{1/2} + \sin^{-1} m(1 - \bar{q}/2) / [1 + m^2(1 - \bar{q}/2)^2]^{1/2} \} \} - [1 + m^2(1 - \bar{q})]^{3/2} - 1 + (m^2/\kappa)(C_f/2) \times [1 + m^2(1 - \bar{q})\bar{q}/2] \quad (9)$$

where  $\bar{u}_m$  is obtained from matching derivatives and, upon simplification, can be expressed as

$$\bar{u}_m = \bar{q}/2 + 1/m[1 + m^2(1 - \bar{q}/2)^2]^{1/2} \times \sin \{ \frac{1}{2} \sin^{-1} m(1 - \bar{q}/2) / [1 + m^2(1 - \bar{q}/2)^2]^{1/2} - \frac{1}{2} \sin^{-1} m(\bar{q}/2) / [1 + m^2(1 - \bar{q}/2)^2]^{1/2} - m/2\kappa(C_f/2)^{1/2} \ln[1 + m^2(1 - \bar{q})] \} \quad (10)$$

Note that for  $\bar{q} = 1$ , the case of equal heat transfer or equal wall temperature treated in Ref. 1, the bracketed term in Eq. (10) vanishes so that  $\bar{u}_m = \frac{1}{2}$  and the flow above the midpoint,  $y_m/d = \frac{1}{2}$ , is the reverse image of that below the midpoint.

In summary, for a given Mach number,  $M_\infty$ , Reynolds number,  $Re_d$ , and stationary wall heat flux,  $\bar{q}$ , the skin-friction coefficient for either wall,  $C_f$ , and the velocity at the matching point,  $u_m$ , are given by Eqs. (9) and (10), and with these values, the velocity profile is given by Eqs. (7) and (8). The corresponding density or enthalpy distributions can then be obtained from Eq. (6).

Sample results are given for  $E = 8.8$ ,  $\kappa = 0.4$  and  $Pr_\epsilon = 1$ . Velocity profiles for an adiabatic stationary wall and various Mach numbers are shown in Fig. 2 along with low-speed experimental data of Robertson<sup>2</sup> with which the calculated  $M_\infty = 0$  profile compares favorably. The difference in  $Re_d$  from  $10^5$  to  $0.6 \times 10^6$  (that of the data taken from Ref. 2) accounts for such a small shift in the velocity profile that it does not affect the comparison.

The influence of the stationary wall enthalpy on skin-friction and heat-transfer coefficients for  $M_\infty = 4$  and various Reynolds numbers is shown in Fig. 3. The heat rates at both walls can be calculated from the relations

$$q_w = C_H \rho_\infty U_\infty (h_w - h_r) = -\frac{1}{4} \bar{q} C_f \rho_\infty u_\infty^3,$$

$$q_\infty = \frac{1}{2} (1 - \bar{q}/2) C_f \rho_\infty u_\infty^3$$

### References

- <sup>1</sup> Korkegi, R. H. and Briggs, R. A., "On Compressible Turbulent Plane Couette Flow," *AIAA Journal*, Vol. 6, No. 4, April 1968, pp. 742-744.
- <sup>2</sup> Robertson, J. M., "On Turbulent Plane-Couette Flow," *Proceedings of the 6th Midwestern Conference on Fluid Mechanics*, Univ. of Texas, Austin, 1959, pp. 169-182.
- <sup>3</sup> Spalding, D. B. and Chi, S. W., "The Drag of a Compressible Turbulent Boundary Layer on a Smooth Flat Plate with and without Heat Transfer," *Journal of Fluid Mechanics*, Vol. 18, Pt. 1, Jan. 1964, pp. 117-143.
- <sup>4</sup> Korkegi, R. H. and Briggs, R. A., "The Hypersonic Slipper Bearing—A Test Track Problem," *Journal of Spacecraft and Rockets*, Vol. 6, No. 2, Feb. 1969, pp. 210-212.

## Numerical Quadrature and Radiative Heat-Transfer Computations

D. C. LOOK JR.\*

University of Missouri, Rolla, Mo.

AND

T. J. LOVE†

University of Oklahoma, Norman, Okla.

### Nomenclature

$B(x), B(y)$	= nondimensional radiosity of one variable
$B(x, y), B(\xi, \eta)$	= nondimensional radiosity of two variables
$B_r(x)$	= convergent nondimensional radiosity value from Ref. 2 for infinite adjoint plates
$x, y, \xi, \eta$	= normalized independent variable
$\rho$	= reflectance
$K(x, y), K(x, y, \xi, \eta)$	= kernels of the integral equations
$W_i$	= weighting coefficients of the numerical quadrature method
$Z_1$	= artificial parameter for one variable geometry
$Z_2$	= artificial parameter for two variable geometry
$n$	= order of quadrature or number of intervals associated with a numerical quadrature method
$\theta$	= angular separation of infinite adjoint plates
$E$	= approximate percentage error between $B(x)$ and $B_r(x)$

Received November 3, 1969; revision received January 5, 1970.

\* Assistant Professor, School of Mechanical and Aerospace Engineering. Member AIAA.

† Director, School of Aerospace and Mechanical Engineering. Member AIAA.

THE integral equations involved in radiative heat-transfer computations usually do not lend themselves to exact analytical solutions. Numerical quadrature are thus often used to obtain approximate solutions. The question of the validity of the quadrature selected must be considered. That is, some precaution must be taken in applying a numerical quadrature to the integral equation involved.

Consider the nondimensional form of the equation for the radiosity of a diffuse gray enclosure in terms of a single variable (Ref. 1, p. 81)

$$B(x) = 1 + \rho \int B(y) K(x, y) dy \quad (1)$$

An approximate solution may be obtained by the substitution of numerical quadrature for the integral in Eq. (1). Thus

$$B(x_i) = 1 + \rho \sum_{j=0}^n W_j B(x_j) K(x_i, x_j) \quad (2)$$

Equation (2) may be rearranged to the form

$$1 = [1 - \rho W_i K_{ii}] B_i - \rho \sum_{\substack{j=0 \\ i \neq j}}^n B_j K_{ij} W_j \quad (3)$$

where  $B_i = B(x_i)$ ,  $K_{ij} = K(x_i, x_j)$ . Since all the quantities in Eq. (3) are positive, mathematically plausible approximate solutions are available if and only if

$$Z_1 = 1 - \rho K_{ii} W_i > 0 \quad (4)$$

If, for example, the trapezoidal rule is to be used,  $W_0 = W_n = 1/2n$  and  $W_1 = \dots = W_{n-1} = 1/n$  where  $x_i = -\frac{1}{2} + i/n$ ,  $0 \leq i \leq n$ . It is easily seen that as  $n$  increases,  $W_i$  approaches zero and depending on the form of  $K_{ii}$ , Eq. (4) may become valid and  $Z_1$  will approach one. Applying this example to the problem of plane parallel plates of infinite length (Fig. 1a), Eq. (4) takes the form

$$Z_{11} = 1 - \rho/2nH > 0 \quad (5)$$

Also applying this example to plane adjoint plates of infinite length (Fig. 1b), Eq. (4) takes the form

$$Z_{12} = 1 - (\rho/4nx_i) \cot(\theta/2) \cos(\theta/2) > 0 \quad (6)$$

Notice that Eq. (5) indicates the selection of  $n$  is such that  $n > \rho/2H$ , while Eq. (6) indicates  $n > (\rho/4x_i) \cot(\theta/2) \cos(\theta/2)$ . Thus, the trapezoidal rule may be easily applied to the parallel plates case, but will introduce large error in the adjoint plates case.

Gaussian quadrature may be applied to the adjoint plates case but only very carefully as may be seen by Table 1. The parameter  $Z$  has been included in this table to illustrate its usefulness. It may be noted that as the parameter  $Z$  approaches one, the approximate percentage error approaches zero. This indicates that if the parameter  $Z$  is greater than zero, no negative radiosities occur and as the value of

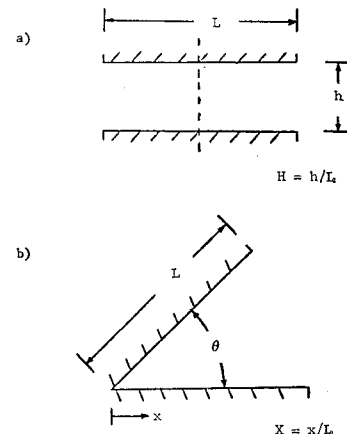


Fig. 1 Geometry of infinite length plates: a) parallel and b) adjoint.